

# Improved gauge action on an anisotropic lattice II

## - Anisotropy parameter in the medium coupling region -

S. Sakai<sup>a</sup> and A. Nakamura<sup>b</sup>

<sup>a</sup>*Faculty of Education, Yamagata University, Yamagata 990-8560, Japan*

<sup>b</sup>*RIISE, Hiroshima University, Higashi-Hiroshima 739-8521, Japan*

---

### Abstract

The quantum correction of the anisotropy parameter,  $\eta$ , is calculated for  $\xi = 2$  and 3 in the  $\beta$  region where numerical simulations such as hadron spectroscopy are currently carried out, for the improved actions composed of plaquette and rectangular 6-link loops. The  $\beta$  dependences of  $\eta$  for the renormalization group improved actions are quite different from those of the standard and Symanzik actions. In Iwasaki and DBW2 actions,  $\eta$  stays almost constant in a wide range of  $\beta$ , which also differs from the one-loop perturbative result, while in the case of Symanzik action, it increases as  $\beta$  decreases, which is qualitatively similar to the perturbative result, but the slope is steeper. In the calculation of the  $\eta$  parameter close to and in the confined phase, we have applied the link integration method to suppress the fluctuation of the gauge fields. Some technical details are summarized.

---

## 1 Introduction

Anisotropic lattices, with temporal lattice spacing smaller than the spatial one, provide an effective method of precise Monte Carlo calculations of, for example, heavy quark systems, glueball masses, finite temperature properties of the QCD. Properties of the anisotropic lattice with the standard plaquette action have been studied by several groups[1,2,3].

On the other hand, improved actions are proposed to obtain numerical results close to the continuum limit on relatively coarse lattices. Therefore it is worth studying the anisotropic properties of the improved actions.

In the previous paper, we studied the anisotropic lattice for a class of improved actions in the weak coupling region, mainly using the perturbative method[4]. The improved actions we considered are written in terms of the plaquette and 6-link rectangular loops as

$$S \propto \sum [C_0 P(1 \times 1)_{\mu\nu} + C_1 P(1 \times 2)_{\mu\nu}], \quad (1)$$

where  $C_0$  and  $C_1$  satisfy the relation  $C_0 + 8C_1 = 1$ . The improved actions frequently used in the simulations correspond to the following parameters:  $C_1 = -1/8$  (Symanzik's improved action[6]),  $C_1 = -0.331$  (Iwasaki's improved action[5]), and  $C_1 = -1.4088$  (QCDTARO's DBW2 action[7]).

For these types of actions, we can formulate the anisotropic lattice in the same way as the standard plaquette action,

$$S_g = \beta_\xi \left( \frac{1}{\xi_B} \sum_x \sum_{i>j} P_{ij} + \xi_B \sum_x \sum_{i \neq 4} P_{4i} \right), \quad (2)$$

where  $\beta_\xi = \sqrt{\beta_\sigma \beta_\tau}$ , and  $\xi_B$  is a bare anisotropic parameter which controls the anisotropy in the space and time directions. The anisotropy is defined as the ratio of the lattice spacing in the spatial ( $a_\sigma$ ) and the temporal ( $a_\tau$ ) directions,  $\xi_R = a_\sigma/a_\tau$ .

Due to quantum correction,  $\xi_R$  is not equal to  $\xi_B$ . Therefore it is essential to know their relationship before large scale simulations on the anisotropic lattice with improved actions are carried out.

The effects of quantum correction have been studied using the parameter  $\eta$  defined by

$$\eta = \frac{\xi_R}{\xi_B}. \quad (3)$$

In the weak coupling region, it is calculated perturbatively[1],[4]. The one-loop perturbative results have been very impressive in the sense that as  $-C_1$  increases, qualitative change is observed in the behavior of  $\eta$  as a function of  $\beta$ . If it is parametrized as

$$\eta(\xi, \beta, C_1) = 1 + \frac{N_c}{\beta} \eta_1(\xi, C_1), \quad (4)$$

the coefficient  $\eta_1$  decreases as  $-C_1$  increases, and at around  $C_1 \sim -0.18$ , it reaches to zero and then becomes negative. Therefore  $\eta(\beta)$  of Iwasaki action

and DBD2 action decreases as  $\beta$  decreases, while in the case of the standard and Symanzik actions, it increases. Namely, they have opposite  $\beta$  dependences.

The natural question is what would be the behavior of  $\eta$  in the smaller  $\beta$  region, where the perturbative calculation breaks down. In this work, we will focus on the  $\eta$  parameter at  $\xi_R = 2$  and 3, and calculate it in the intermediate  $\beta$  region where most current numerical simulations are carried out.

In Section 2, we discuss appropriate regions of  $\beta$  for the improved actions to evaluate  $\eta$ , and explain some details of the calculation: matching of the lattice potential in the spatial and temporal directions, and the method of eliminating the effects of self-energy terms of lattice potential on an anisotropic lattice. For the standard action, the effect of the self-energy terms on  $\eta$  has been studied by the Bielefeld group [3]. They reported that the effects on  $\eta$  are small about 1% throughout the parameter range that they studied. We discuss the effects for improved actions and show, in Section 3, that they are not large.

In Section 3,  $\eta$  for each improved action is presented. The  $\eta$  behavior in the intermediate  $\beta$  region is quite different for each improved action. Iwasaki and DBW2 actions are qualitatively different in the one-loop perturbative calculation.

Section 4 is devoted to the discussion and conclusion. It is found that for Iwasaki action,  $\eta$  is close to unity in the region  $\beta \geq 2.5$ , indicating that the detailed calibration of  $\xi_B$  for a given  $\xi_R$  is not important unless a very precise simulation is carried out. For DBW2 action,  $\eta$  remains essentially constant, indicating that rough calibration gives a reasonable estimation of  $\eta$ . For Symanzik action some detailed calculation of  $\eta$  is necessary, as in the case of standard action.

For the calculation of the  $\eta$  parameter, measurements of the large Wilson loops are required. Large Wilson loops suffer from huge fluctuation of the gauge fields, particularly in the confined phase. To suppress the fluctuation, the link integration method has been proposed [8,9,10]. In this work, we have applied the link integration method in small  $\beta$  regions. Here, it is very important to choose an adequate radius (optimal radius) of integration in the complex plane. For the standard action, the optimal radius was studied by the Bielefeld Group [3]. In appendix A, we describe the optimal radii for Symanzik and Iwasaki actions.

## 2 Calculation of the anisotropy quantum correction, $\eta$

### 2.1 Region of coupling constant to be studied

In this work, we calculate the  $\eta$  parameter in the regions of  $\beta$  where most numerical calculations are currently carried out. In the case of standard action, hadron spectroscopy in the quench approximation has been reported for  $5.7 < \beta < 6.2$  [11]. In these coupling constant regions, the light hadron masses are reproduced within 10% accuracy, which may be the limit of the quench approximation. Therefore, we calculate the  $\eta$  parameter around these lattice spacings for the improved actions.

In order to estimate the lattice spacing for the improved actions, we use the critical  $\beta$  ( $\beta_{Crit}$ ) of finite temperature transition. For standard action,  $\beta = 6.05$  corresponds to the finite temperature transition point of the  $N_T = 8$  lattice[12]. Therefore we estimate  $\beta_{Crit}$  at  $N_T = 8$  for the improved actions. For tree level improved Symanzik action,  $\beta_{Crit}$ 's are reported for  $N_T = 3, 4, 5$  and  $6$ [13], and for Iwasaki action, they have been calculated at  $N_T = 4, 6$  by the Tsukuba group[14] and at  $N_T = 8$ , by the Yamagata-Hiroshima collaboration[15]. For DBW2 action, they are reported by the QCDTARO collaboration[7] for  $N_T = 3, 4$  and  $6$ .

$\beta_{Crit}$  at  $N_T = 8$  is estimated using the two loop asymptotic scaling relation for lattice spacing,

$$a = \frac{1}{\Lambda} \left( \frac{6b_0}{\beta} \right)^{-c} \exp\left(-\frac{\beta}{12b_0}\right), \quad (5)$$

where  $a$  is the lattice spacing and  $c = b_1/(2b_0^2)$ , with  $b_0 = 11/(4\pi)^2$  and  $b_1 = 102/(4\pi)^4$ . We applied two methods for the estimation of  $\beta_{Crit}$  at  $N_T = 8$ . In method 1, we use  $\beta_{Crit}$  at  $N_T = 6$  of the same action to estimate  $\beta_{Crit}(N_T = 8)$  using  $T_c = 1/(aN_T)$ . In method 2, we use the  $\beta_{Crit}(N_T = 8)$  of the standard action to evaluate  $\beta_{Crit}(N_T = 8)$  of the other action with the  $\Lambda$  parameter[4,16]. They are summarized in the table 1.

In the case of Symanzik action, the estimations of  $\beta_{Crit}$  by the two methods

Table 1

Estimation of  $\beta_{Crit}$  at  $N_T = 8$  for various actions

	$\beta_{Crit}(data)$	Method 1	Method 2	Minimum $\beta$
<i>Standard</i>	6.05( $N_T = 8$ )			
<i>Symanzik</i>	4.31( $N_T = 6$ )	4.57	4.56	4.5
<i>Iwasaki</i>	2.52( $N_T = 6$ )	2.78	2.32	2.5
<i>DBW2</i>	0.936( $N_T = 6$ )	1.28	-	1.1

coincide with each other. For Iwasaki action, some discrepancy is observed

between the two estimations. The first method gives a closer result to that of Ref.[15], in which  $\beta_{Crit} = 2.73 \sim 2.75$ .

For DBW2 action,  $\beta_{Crit}$  estimated using the  $\Lambda$  ratio becomes negative. In this  $\beta$  region, the deviation from the perturbative scaling relation is quite large for this action. Therefore, for the estimation of  $\beta_{Crit}(N_T = 8)$ , we plot  $\beta_{Crit}$  at  $N_t = 3, 4$  and  $6$  and simply extrapolate it. It becomes about  $\beta = 1.1$  with large ambiguity. Therefore we will study the action until  $\beta = 1.0$ .

In the table 1, we show also the minimum of  $\beta$ , for which we calculate the  $\eta$  parameters.

## 2.2 Subtraction of the self-energy contribution from the lattice potential

The renormalized anisotropy  $\xi_R$  is defined as the ratio of the lattice spacings in the spatial and temporal directions,  $\xi_R = a_\sigma/a_\tau$ . In the quench approximation, the lattice potential has been used as the probe of lattice spacing, and is defined as the ratio of Wilson loops,

$$V(p, r) = \log\left(\frac{W(p, r)}{W(p+1, r)}\right). \quad (6)$$

The lattice potentials in the spatial ( $V_s$ ) and temporal directions ( $V_t$ ) are determined by the Wilson loops in the space-space plane and the space-time plane, respectively. The lattice potential defined in Eq.6 will become independent of the position  $p$  when  $p$  becomes large where the lattice artifact disappears. In the following, we will discard  $p$  in the artifact-free region, but write it explicitly when we discuss its effect.

The matching of the potential in the spatial and temporal directions [2,17] has been used for the determination of  $\xi_R$  as

$$V_s(\xi_B, r) = V_t(\xi_B, t = \xi_R \times r). \quad (7)$$

In the calculation of  $\eta$ , we fix the renormalized anisotropy  $\xi_R$ , and then search for the point of  $\xi_B$  where the Eq.7 is satisfied [2]. Using these  $\xi_B$  and  $\xi_R$  values, the  $\eta$  parameter is calculated.

The lattice potential defined by Eq. 6 suffers from the self-energy term. In this article, we assume the simplest parameterization for it:

$$V_s(\xi_B, r) = V_s^0(\xi_B) + V_s^L(\xi_B, r), \quad (8)$$

where  $V_s^L$  is the lattice potential free of self-energy contributions. The temporal potential,  $V_t(\xi_B, t)$ , is treated similarly. On an anisotropic lattice,  $V_s^0(\xi_B)$  and  $V_t^0(\xi_B)$  may be different from each other due to the anisotropy. Therefore the matching of the potential should be applied for the self-energy-free parts,  $V_s^L$  and  $V_t^L$ .

In order to eliminate the effect of the self-energy term  $V^0$ , we define the subtracted potential:

$$V_s^{Sub}(\xi_B, r, r_0) = V_s(\xi_B, r) - V_s(\xi_B, r_0) = V_s^L(\xi_B, r) - V_s^L(\xi_B, r_0). \quad (9)$$

$V_t^{Sub}$  is defined in a similar manner.

The subtraction points  $r_0$  and  $t_0$  are chosen to satisfy  $t_0 = \xi_R r_0$ , and the matching of the potential,  $V_t^L(t_0 = \xi_R r_0) = V_s^L(r_0)$ , should also be satisfied there. Namely, at  $r_0$ , the lattice potential should be free of the lattice artifacts. This condition is satisfied if  $r_0$  is large. At large  $r_0$ , however, the fluctuation of the potential increases, and simulations with high statistics on a larger lattice are required. Therefore,  $r_0$  should be chosen to be as small as possible, where the lattice artifacts will be sufficiently small.

### 2.3 Matching method

As an example, we will show details of the determination of  $\eta$  in the case of Iwasaki action at  $\beta = 4.5$ ,  $\xi_R = 2$  on the  $12^3 \times 24$  lattice.

Let us start with the determination of the subtraction point  $r_0$ . In order to reduce statistical error, small  $r_0$  is preferable. In the small  $r_0$  region, however, systematic error due to lattice artifacts becomes large. The optimal choice of  $r_0$  requires careful study by trial and error.

First we calculate the ratio

$$R(\xi_B, p, r) = \frac{V_s(\xi_B, p, r)}{V_t(\xi_B, p, t = \xi_R \times r)}, \quad (10)$$

where  $V_s$  and  $V_t$  mean the lattice potential in the space and time directions, respectively, and include the self-energy contributions. Our results are displayed in the Fig. 1. As  $r$  increases, the ratio  $R(p, r)$  approaches an asymptotic value. It is seen that at  $r = 1$ , the deviation from the asymptotic value is rather large, which may be due to lattice artifacts. Therefore, we first choose  $r_0 = 3$ , and calculate the subtracted potentials of Eq.9, and then use them in Eq.10 to obtain ratio  $R$ .

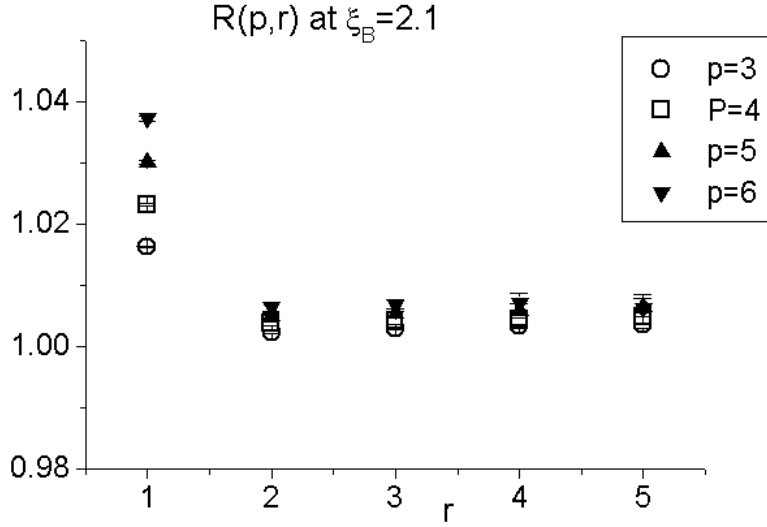


Fig. 1. Ratios given by Eq.10.

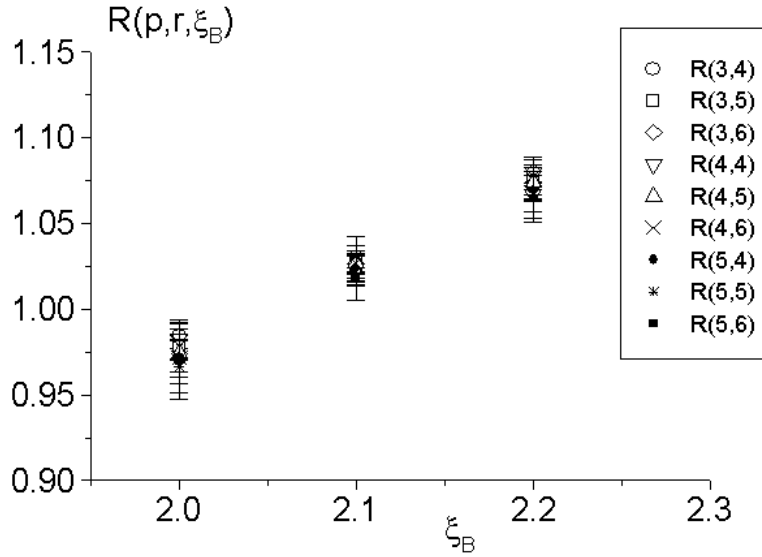


Fig. 2.  $\xi_B$  dependences of the ratios for the subtracted potentials.

The results for  $\xi_B = 2.0, 2.1$  and  $2.2$  are shown in Fig.2. The ratios are shown individually for each  $p$  and  $r$ . We proceed to look for the point where the ratios satisfy the relation  $R(p, r, \xi_B) = 1$ . We fit the three points by the second-order polynomial of  $\xi_B$  and find the solution

$$R(p, r, \xi_B) = c_0 + c_1 \xi_B + c_2 \xi_B^2 = 1. \quad (11)$$

The coefficients  $c_0, c_1$  and  $c_2$  are determined by the three data points of

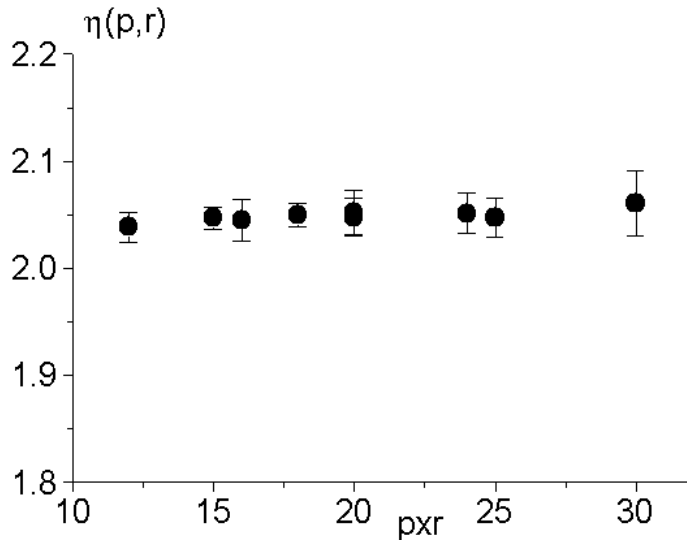


Fig. 3.  $\eta = \xi_R/\xi_B$  at each  $p$  and  $r$ , where  $\xi_R$  ( $\xi_B$ ) stands for the renormalized (bare) anisotropy.

$R(p, r, \xi_B)$ . Using the solution of Eq.11, the ratios  $\eta = \xi_R/\xi_B$  are determined for each  $p$  and  $r$  and are shown in Fig.3.

In order to avoid the lattice artifact, we choose the data with  $p \geq 3$  and  $r \geq 4$ . In this region,  $\eta(p, r)$  is almost independent of  $p$  and  $r$ .  $\eta$  at this  $\beta$  is determined as the average of the data. The errors are estimated by the jackknife method; the data after thermalization is grouped into 10 blocks and they are used as independent data. In this way the result becomes  $\eta = 0.9766 \pm 0.0044$  when  $r_0 = 3$ .

The same analysis is carried out by taking  $r_0 = 2$ . The result becomes  $\eta = 0.9764 \pm 0.0039$ . The result changes little in this case. However, if we choose  $r_0 = 1$ , the results differ significantly from those of  $r_0 = 2$  and 3. Analyses are carried out at other values of  $\beta$  and  $\xi$ . There are several cases in which a slight difference is observed between  $r_0 = 2$  and  $r_0 = 3$ . Therefore in the case of Iwasaki action, we choose  $r_0 = 3$  for all values of  $\beta$  and  $\xi_B$  in this work.

We carried out the same studies for Symanzik and DBW2 actions. In these cases, the subtraction point becomes  $r_0 = 4$ . This indicates that lattice artifacts are larger for these actions.



### 3 Result for the quantum correction of the anisotropy, $\eta$

#### 3.1 Simulation parameters, numerical results and self-energy contribution

The simulations are mainly carried out on the  $12^3 \times 12\xi_R$  lattice. For some values of  $\beta$  and  $\xi$ , a larger  $16^3 \times 16\xi_R$  lattice is employed in order to study the size dependence. It is found that the lattice size effect is small.

The gauge configurations are generated by the heat bath method with over-relaxation [18,19]. Typical numbers of the Monte Carlo (MC) data for the calculation of  $R(\xi_B, p, r)$  are a few tens of thousand after thermalization of about  $10^4$  MC sweeps. However, as  $\beta$  decreases and approaches the finite transition point or goes into the confined phase, both the necessary number of MC data and the number of thermalization sweeps increase. For the calculation of  $\eta(\xi = 2)$  at  $\beta = 2.5$  for Iwasaki action, we used  $1.5 \times 10^6$  data after thermalization of  $3.5 \times 10^5$  MC sweeps.

In order to suppress the fluctuation of the gauge fields in the calculation of large Wilson loops, we applied the link integration method [9,10]. It is used for the calculation of the lattice potentials at  $\beta = 2.5$  and  $2.56$  for Iwasaki action and  $\beta = 4.5$  for Symanzik action. Technical details will be presented in the appendix. Here we only notice that, in the case of improved actions, the effect of the link integration is reduced due to the presence of the rectangular 6-link loops.

Our results of  $\eta$  are summarized in the tables 2 to 7. In order to show the effects of self energy terms in the lattice potential, we have presented the results for  $\eta$ , which are obtained without subtracting the self energy terms in the  $\eta^{Nosub}$  column in these tables. It is found that the difference between them is less than  $\sim 1\%$  for Symanzik and Iwasaki actions. This is consistent with the result for the standard action obtained by Bielefeld group[3]. However, for DBW2 action, the difference increases. It amounts to a few percent but is still small. Therefore, except for the case of the simulation with a few percent accuracy, it is safe to use  $\eta^{Nosub}$ , which has been reported at the XVIIth International Symposium on Lattice Field Theory at Pisa (Lattice '99) [21].

#### 3.2 Symanzik action

In Fig.4, we show the values of the  $\eta$  parameter as a function of  $\beta$  for Symanzik action. The qualitative behavior of  $\eta$  as a function of  $\beta$  is the same

Table 2

$\eta \equiv \xi_R/\xi_B$  for Symanzik action at  $\xi_R = 2$ , where  $\xi_R$  and  $\xi_B$  are the renormalized and bare anisotropies, respectively. At  $\beta = 8.0$  and  $4.5$  the simulation is carried out on  $16^3 \times 32$  lattice to study the size dependences. They are shown in the line with the symbol  $*$ .

Symanzik Action at  $\xi_R = 2$ 

$\beta$	$\eta$	$\eta^{NoSub}$
10.0	$1.0227 \pm 0.0097$	$1.0271 \pm 0.0031$
8.0	$1.0393 \pm 0.0191$	$1.0391 \pm 0.0020$
6.0	$1.0381 \pm 0.0097$	$1.0500 \pm 0.0029$
4.5	$1.0980 \pm 0.0255$	$1.1011 \pm 0.0021$
8.0*	$1.0284 \pm 0.0021$	$1.0232 \pm 0.0039$
4.5*	$1.1095 \pm 0.0122$	$1.1040 \pm 0.0062$

Table 3

$\eta$  as a function of  $\beta$  for Symanzik action at  $\xi_R = 3$ .

Symanzik Action at  $\xi_R = 3$ 

$\beta$	$\eta$	$\eta^{NoSub}$
10.0	$1.0341 \pm 0.0146$	$1.0426 \pm 0.0058$
8.0	$1.0260 \pm 0.0150$	$1.0361 \pm 0.0042$
6.0	$1.0520 \pm 0.0200$	$1.0667 \pm 0.0015$
4.5	$1.1482 \pm 0.0317$	$1.1331 \pm 0.0064$

Table 4

$\eta$  for Iwasaki action at  $\xi_R = 2$ . The data for  $\beta = 3.5$  with  $*$  are calculated on the  $16^3 \times 32$  lattice to study the size dependences.

Iwasaki Action at  $\xi_R = 2$ 

$\beta$	$\eta$	$\eta^{NoSub}$
10.0	$0.9811 \pm 0.0030$	$0.9742 \pm 0.0033$
6.0	$0.9831 \pm 0.0037$	$0.9784 \pm 0.0032$
4.5	$0.9755 \pm 0.0083$	$0.9776 \pm 0.0044$
4.0	$0.9806 \pm 0.0074$	$0.9782 \pm 0.0039$
3.5	$0.9761 \pm 0.0105$	$0.9767 \pm 0.0049$
3.05	$0.9911 \pm 0.0182$	$0.9881 \pm 0.0060$
2.5	$0.9998 \pm 0.0045$	$0.9837 \pm 0.0074$
3.5*	$0.9803 \pm 0.0070$	$0.9891 \pm 0.0036$

in perturbative and numerical results. However, the slope of  $\eta$  becomes steeper for the numerical results.

Table 5  
 $\eta$  for Iwasaki action at  $\xi_R = 3$ .

Iwasaki Action at  $\xi_R = 3$

$\beta$	$\eta$	$\eta^{NoSub}$
10.0	$0.9714 \pm 0.0054$	$0.9647 \pm 0.0006$
6.0	$0.9569 \pm 0.0041$	$0.9554 \pm 0.0026$
4.0	$0.9700 \pm 0.0118$	$0.9645 \pm 0.0063$
3.5	$0.9715 \pm 0.0160$	$0.9708 \pm 0.0031$
3.05	$0.9725 \pm 0.0120$	$0.9776 \pm 0.0037$
2.56	$1.0011 \pm 0.0138$	$1.0011 \pm 0.0071$

Table 6  
 $\eta$  as a function of  $\beta$  for DBW2 action at  $\xi_R = 2$ .

DBW2 action at  $\xi_R = 2$

$\beta$	$\eta$	$\eta^{NoSub}$
2.5	$0.9084 \pm 0.0090$	$0.8626 \pm 0.0025$
1.6	$0.9011 \pm 0.0082$	$0.8616 \pm 0.0018$
1.4	$0.8917 \pm 0.0122$	$0.8623 \pm 0.0024$
1.2	$0.8882 \pm 0.0115$	$0.8673 \pm 0.0032$
1.1	$0.8868 \pm 0.0144$	$0.8753 \pm 0.0030$
1.0	$0.8781 \pm 0.01069$	$0.8817 \pm 0.0092$

Table 7  
 $\eta$  for DBW2 action at  $\xi_R = 3$ .

DBW2 action at  $\xi_R = 3$

$\beta$	$\eta$	$\eta^{NoSub}$
1.4	$0.8283 \pm 0.0189$	$0.8082 \pm 0.0046$
1.2	$0.8157 \pm 0.0252$	$0.8070 \pm 0.0055$
1.1	$0.8122 \pm 0.0230$	$0.8210 \pm 0.0076$
1.0	$0.8123 \pm 0.0235$	$0.8262 \pm 0.0101$

In this case the tadpole improved one-loop perturbation calculation (boosted perturbation) [22,23] reduces the discrepancy. It may be to replace  $\beta$  in Eq. 4 by  $\tilde{\beta} = \beta \sqrt{W_s(1, 1)W_t(1, 1)}$ :

$$\eta(\xi, \beta) = 1 + \frac{N_c}{\beta} \frac{\eta_1(\xi)}{\sqrt{W_s(1, 1)W_t(1, 1)}}. \quad (12)$$

In this formula, since  $W_s(1, 1)$  and  $W_t(1, 1)$  decrease as  $\beta$  decreases, the  $\beta$  dependence of  $\eta$  is more enhanced. The use of Eq.12 improves the agreement

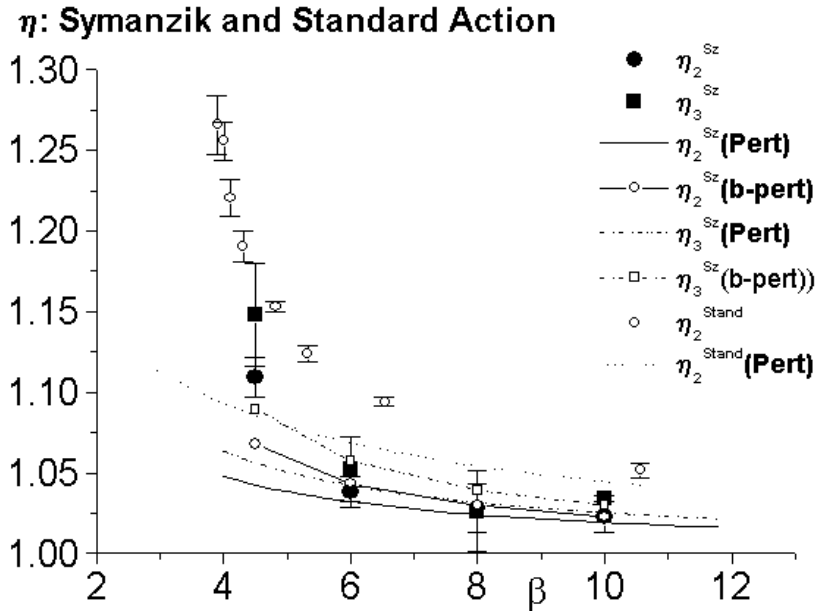


Fig. 4.  $\eta$ s for Symanzik ( $\eta^{Sz}$ ) and standard ( $\eta^{Stand}$ ) actions. For standard action, we show the results obtained by Klassen[2].  $\beta$  of standard action is shifted by Eq.5, in order to compare the  $\eta$  at the same lattice spacing  $a$ . The perturbative results are also shown for comparison with numerical results. The  $\eta(b-pert)$  represents the boosted perturbation result(Eq. 12).

between perturbative and numerical results a little as shown in the Fig. 4.

In this figure, we also show the result from the standard plaquette action[2]. In order to compare  $\eta$  at the same lattice spacing, we have shifted  $\beta$  of standard action to that of Symanzik action using the asymptotic scaling relation Eq. 5. Because the two estimations coincide for Symanzik action for  $\beta_{Crit}$  at the  $N_T = 8$  lattice in Section 2.1, in these regions the asymptotic scaling relation Eq.5 may be satisfied at least approximately for these two actions. It is found that the qualitative behaviors are the same, although the slope becomes more gentle for Symanzik action.

### 3.3 Iwasaki Action

Results for Iwasaki action are shown in Fig.5.  $\eta_2$  exhibits a shallow dip around  $\beta \sim 4.5$  and then increases with decreasing  $\beta$ .  $\eta_3$  shows similar behavior, but the position of the dip moves to  $\beta \sim 6.0$ . Both  $\eta_2$  and  $\eta_3$  stay close to unity in a wide range of  $\beta$  for  $\beta \geq 2.5$ . The deviation from unity is more enhanced for  $\eta_3$ .

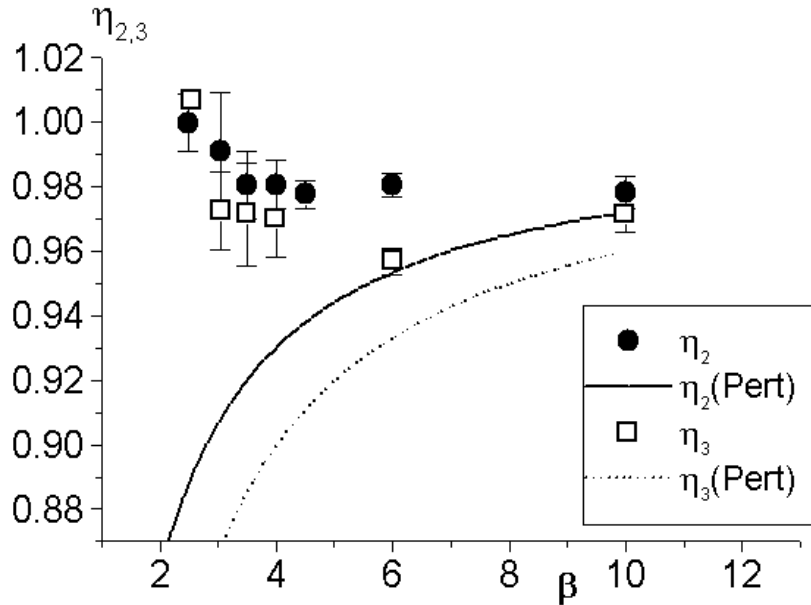


Fig. 5.  $\eta$  for Iwasaki action.

In the continuum limit, the  $\eta$  parameter approaches one. The improved action has an  $\eta$  value that remains one in a wide range of  $\beta$ ;  $2.5 \leq \beta$ . The deviation from unity is within 4% when  $\xi_R = 2$ , and 3, therefore until precision simulation of a few % accuracy is required, detailed calibration of  $\eta$  is not necessary. This is a good property for simulations.

For Iwasaki action, the one-loop perturbative calculation predicts a monotonic decrease in  $\eta$  as  $\beta$  decreases[4], as shown in Fig.5. The numerical results are qualitatively different from those of the one-loop perturbation.

### 3.4 DBW2 Action

Results for DBW2 action are shown in Fig.6.  $\eta$  stays almost constant;  $\eta_2 \sim 0.9$  in the range  $1.0 \geq \beta \geq 2.5$  and  $\eta_3 \sim 0.81$  in the range  $1.0 \geq \beta \geq 1.4$ . The deviation from unity is not small in this case, but the flatness of  $\eta$  as a function of  $\beta$  is again a good property for numerical simulations. The rough calibration of  $\eta$  at a few  $\beta$  points is sufficient to obtain a reasonable estimation of  $\xi_B$ . As in the case of Iwasaki action, the numerical results show qualitatively different behavior from the one-loop perturbative ones [4] (see Fig.6).

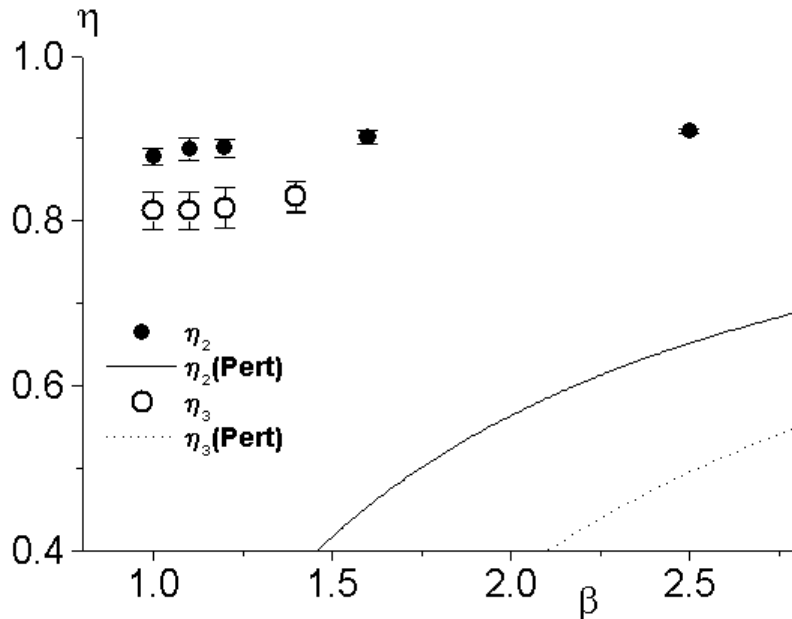


Fig. 6.  $\eta$  for DBW2 action.

#### 4 Discussion and Conclusions

In this work, we studied the global structure of  $\eta$  as a function of  $\beta$  and  $C_1$  for the gauge action given in Eq.1. Overall effects of the improved actions on  $\eta$  are summarized as follows. The plaquette term in the action makes the  $\eta$  parameter increase monotonically as  $\beta$  decreases, while the rectangular terms with  $C_1 < 0$  make  $\eta$  decrease.

At  $C_1 = -1/8$ , the effects of rectangular loops are not so large, and the slope of  $\eta$  is smaller than that in the case of standard action. As a result, at the same lattice spacing, the effects of the quantum correction are reduced in Symanzik action. In Symanzik and standard actions, the  $\eta$  dependence on  $\beta$  is qualitatively the same between perturbative and numerical results, but slopes are steeper for numerical results.

At  $-C_1 = 0.331$ , the increase in  $\eta$  due to the plaquette term and its suppression by the rectangular loops are almost in balance in a wide range of  $\beta$ ,  $2.5 \leq \beta$ , and  $\eta$  stays close to one. However, the detailed behavior of these effects depends on  $\beta$  and  $\xi_R$ .  $\eta_2$  and  $\eta_3$  decrease from  $\beta = 2.5$ , and exhibit shallow dips at  $\beta \sim 4.5$  and  $\beta \sim 6.0$ , respectively. These behaviors are qualitatively different from the prediction of one-loop perturbative calculation.

At  $-C_1 = 1.4088$ , the effects of the rectangular loop become stronger than those of the plaquette term, and  $\eta$  becomes less than one. It is almost inde-

pendent of  $\beta$  in the range  $1.0 \leq \beta \leq 2.5$ . This is again qualitatively different from the perturbative result.

As  $\xi_R$  increases, the effects of the two terms in the action are more enhanced, and the balance becomes more subtle.

In the continuum limit,  $\eta$  approaches unity. Then Iwasaki action is close to the continuum limit in the region  $2.5 \leq \beta$  for  $\xi_R = 2$  and  $3$ . Particularly around  $\beta \sim 2.5$ ,  $\eta$  is close to unity. This means that the calibration of  $\eta$  is not necessary until high precision simulation is carried out.

In the case of DBW2 action,  $\eta$  is not close to one. Then, as far as  $\eta$  is concerned, it is not close to the continuum limit in this  $\beta$  region. However,  $\eta$  is almost independent of  $\beta$ . This is a good property for the simulation of physical quantities on anisotropic lattices, because the rough calibration of  $\eta$  is sufficient to determine  $\xi_B$  in this action.

For Symanzik action, the deviation of  $\eta$  from unity is remedied compared with standard action, but the slope of  $\eta$  is steep, and it becomes  $\sim 10\%$  at around  $\beta \sim 5.0$ . Therefore detailed calibration of  $\eta$  is necessary.

For the  $\beta$  and  $\xi$  ranges that we have studied, the differences between  $\eta$  and  $\eta^{Nosub}$  are small for all the improved actions. For Symanzik and Iwasaki actions, the difference is  $\sim 1\%$ , and for DBW2 action, it is a few %. Therefore it is safe to use  $\eta^{Nosub}$  except in the case of very precise simulations. This is good news, because the calculation of  $\eta$  requires much CPU time.

Further data on  $\eta$  for larger  $\xi_R$  and smaller  $\beta$  will be reported in the forthcoming publications, because the calculation of  $\eta$  at smaller  $\beta$  and larger  $\xi_R$  requires much more CPU time.

## ACKNOWLEDGMENTS

This work has been done with SX-5 at RCNP and VX-4 at Yamagata University. We are grateful for the members of RCNP for kind supports.

## A Optimal Radius of Integration For Iwasaki and Symanzik Actions

If  $R$  is an external source field for link variable  $U$ , the link integration of  $U$  is given by

$$\langle U \rangle = \frac{1}{Z} \frac{dZ(R)}{dR^\dagger} = \frac{\int D[U] U \exp(\text{Tr}(RU^\dagger + UR^\dagger))}{\int D[U] \exp(\text{Tr}(RU^\dagger + UR^\dagger))} \quad (\text{A.1})$$

where  $Z(R)$  is expressed by the modified Bessel function  $I_1$  [9,10].

$$Z(R) = \oint \frac{dx}{2\pi i} e^{xQ} \frac{1}{z} I_1(2z) \quad (\text{A.2})$$

and

$$z = \left( \frac{P(x)}{x} \right)^{\frac{1}{2}},$$

$$Q = 2\text{Re}(\det(R)),$$

$$P(x) = 1 + x\text{Tr}(RR^\dagger) + \frac{1}{2}x^2 \left[ (\text{Tr}(RR^\dagger))^2 - \text{Tr}((RR^\dagger)^2) \right] + x^3 \det(RR^\dagger). \quad (\text{A.3})$$

Similarly  $dZ(R)/dR$  is written by the modified Bessel function  $I_1$  and  $I_2$  [9,10].

$$\frac{dZ(R)}{dR^\dagger} = \oint \frac{dx}{2\pi i} x e^{xQ} \frac{1}{z} I_1(2z) \frac{\partial Q}{\partial R^\dagger} + \oint \frac{dx}{2\pi i} \frac{e^{xQ}}{P(x)} I_2(2z) \frac{\partial P(x)}{\partial R^\dagger} \quad (\text{A.4})$$

The path of the integration is a closed circle on the complex plane  $x$ . In principle it is arbitrary, but numerical integration requires adequate radius. In the case of the standard action, the adequate radius was studied by Scheideler [24].

The arguments of the modified Bessel functions become rather large and we apply asymptotic expansion. In this article we use Simpson method for the numerical integration, and search for the region of  $r$  and the number of the division  $N$  where  $\langle U \rangle$  is stable against the change of  $r$ .

An example of the  $r$  dependence of a  $\langle U \rangle$  is shown in Fig.A.1. It is found that when the number of the division is  $N = 100$ , there appears some spurious plateaus, which disappear when  $N = 400$ . However there is a region of  $r$  where  $\langle U \rangle$  is stable in the change of  $N$ , which is the optimal region of integration for  $N = 100$ . The optimal region increases a little when  $N = 400$ . In this article we choose  $N = 100$  and proceed to determine the optimal region of  $r$  ( $r^{opt}$ ).



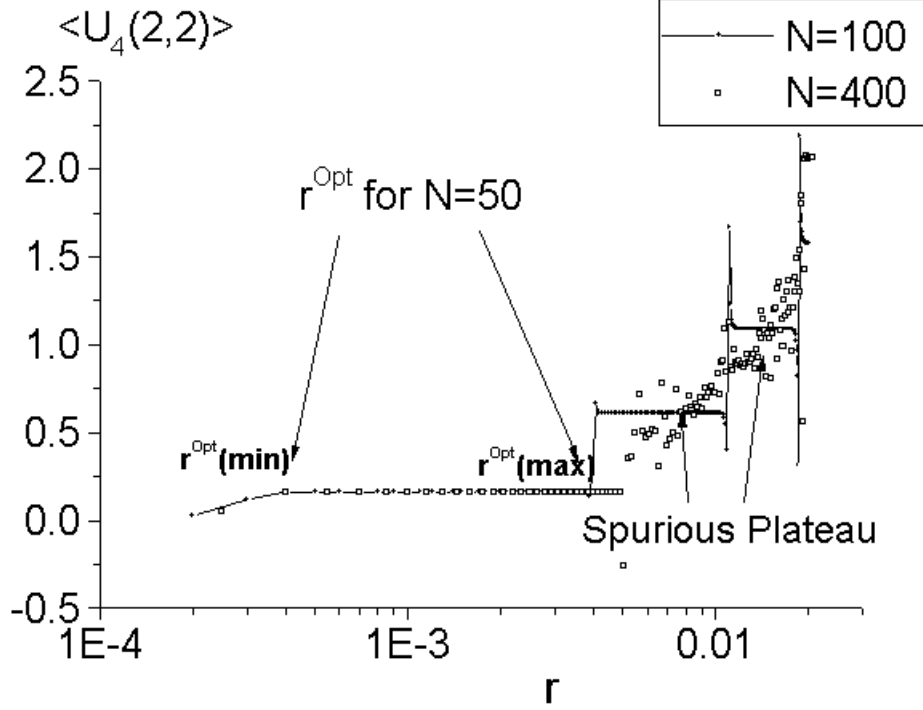


Fig. A.1. Radius dependence of  $\langle U_4(2,2) \rangle$ . The integration is carried out on a configuration of Iwasaki action, fully thermalized at  $\beta = 3.05$  and  $\xi_B = 2.0$ . An integrated link is located at the center of the lattice, directing in the 4-th direction. We have shown the (2,2) elements of the unitary matrix  $U$ .

These plateaus shown in Fig. A.1 are observed when Taylor expansions of the modified Bessel functions are applied. Then they are due to the difficulty in the numerical integrations given by Eq.A.2 and Eq.A.4. Therefore it is important to find the optimal  $r$  region.

For some set of  $\beta$  and  $\xi_B$ , we have obtained the minimum and maximum of  $r^{opt}$  as shown in the Fig. A.1, for space-like and time-like links separately. When  $\xi > 1.0$ ,  $r^{opt}$  of time-like links ( $r_t^{opt}$ ) is smaller than that of space-like links ( $r_s^{opt}$ ). Examples of the difference is shown in the Fig. A.2. It seems that the difference becomes larger as  $\beta$  and  $\xi_B$  increase. The similar properties are observed in the case of standard action.

We proceed to the parameterization of the  $r^{opt}(\beta, \xi)$ . The  $\beta$  and  $\xi$  ranges are  $2.0 \leq \beta \leq 6.0$ ,  $1.8 \leq \xi_B \leq 6.5$  for Iwasaki action and  $4.5 \leq \beta \leq 8.0$ ,  $1.7 \leq \xi_B \leq 5.8$  for Symanzik action. The  $r_{space}^{opt}(min)$  and  $r_{space}^{opt}(max)$  are shown in the Fig. A.3. They decrease with  $\beta$  and  $\xi$  and seems to be parametrized as

$$r^{opt} = a * \exp(-b\beta - c\xi_B) \quad (\text{A.5})$$

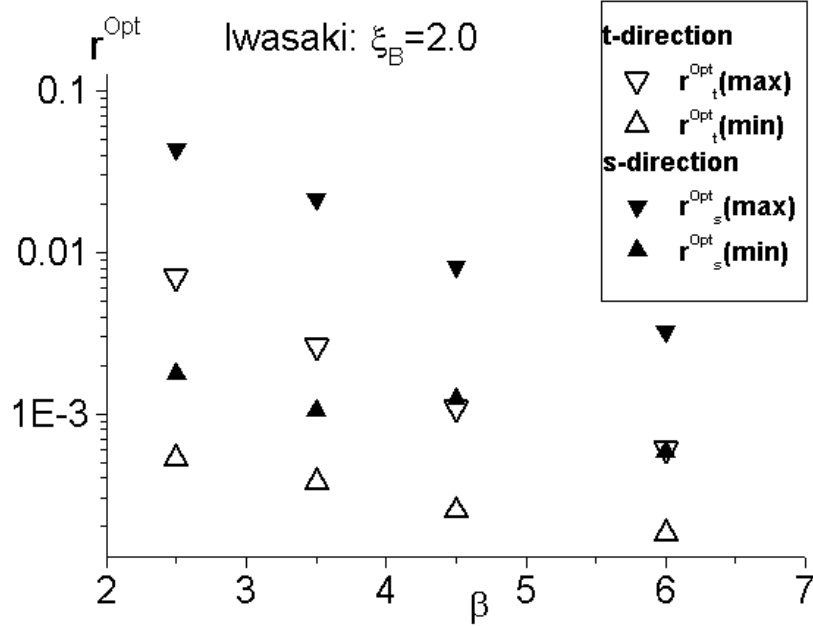


Fig. A.2. Examples of the difference between  $r_{space}^{opt}$  and  $r_{time}^{opt}$  for Iwasaki action at  $\xi_B = 2.0$ .

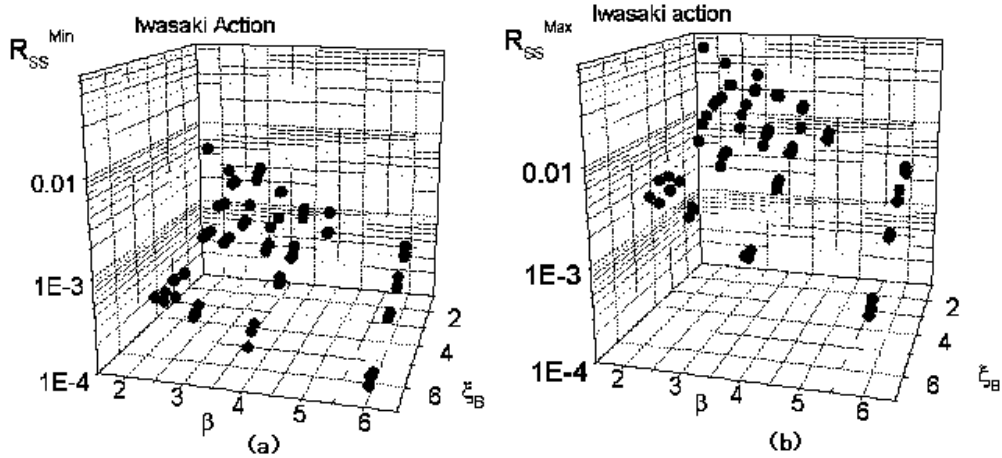


Fig. A.3. A compilation of  $R_{min}$ , (a) and  $R_{max}$  (b) of Iwasaki action in the range  $2.0 \leq \beta \leq 6.0$  and  $2.0 \leq \xi_B \leq 6.0$ .

Then we define  $r^{opt}(mid)$  as,

$$\log(r^{opt}(mid)) = (\log(r^{opt}(min)) + \log(r^{opt}(max)))/2. \quad (\text{A.6})$$

and then fit them by Eq. A.5. For  $\log(r^{opt})$ , it becomes a multiple regression fitting. The coefficients are determined by the least square method. The results for Symanzik and Iwasaki actions are summarized in the table A.1. We

Table A.1

The multiple regression fit of  $r^{opt}(mid)$ . The 60 data and 29 data points are used to determine the coefficients  $a$ ,  $b$ ,  $c$  for Iwasaki and Symanzik actions respectively.

Action		a	b	c
<i>Symanzik</i> (26data)	$r_s^{opt}(mid)$	0.5563	0.5479	0.5336
	$r_t^{opt}(mid)$	0.06244	0.4213	0.6568
<i>Iwasaki</i> (61data)	$r_s^{opt}(mid)$	0.08663	0.5507	0.4315
	$r_t^{opt}(mid)$	0.01682	0.5139	0.5261

have checked that  $r^{opt}(mid)$  with the parameter given by table A.1 is located between  $r^{opt}(max)$  and  $r^{opt}(min)$ ; namely it stays within the optimal radius of integration through out the data points.

$r^{opt}$  region may change with the position of link on a configuration and also with configurations. The results shown in Fig.A.3 are obtained for a link at the center of the configuration in space and time directions, which are fully thermalized. However the fluctuation of the  $r^{opt}$  region is not large. If we choose,  $r^{opt}(mid)$ , it has been in an optimal region of  $r$  for all link variables and configurations.

Let us proceed to discuss the effects of the link integration method. In the case of improved actions, the number of link  $U$  which are simultaneously integrated in a Wilson loop becomes much smaller than the case of standard action, because in the case of improved action the background fields  $R$  of Eq. A.2 extend wider range due to the 6-link rectangular loop in the action. Therefore the effect of link integration method is reduced in these cases, and is not effective for the calculation of smaller Wilson loops.

The example of the suppression of the fluctuation is shown in the Fig. A.4. The suppression of the fluctuation is impressive for  $W(6,6)$  but not for  $W(4,4)$ . The similar properties are observed for the Symanzik action of  $W(8,8)$  and  $W(4,4)$  at  $\eta = 4.5$ . The link integration needs much CPU-time, and therefore the link integration method is effective for the calculation of large Wilson loops in the confined phase or very close to the transition point.

## References

- [1] F. Karsch, Nucl. Phys. B205[FS5] (1982), 285.
- [2] T. R. Klassen, Nucl. Phys. B533 (1998) 557.
- [3] J. Engels, F. Karsch and T. Scheideler, Nucl. Phys. B564 (2000) 303.
- [4] S. Sakai, T. Saito, and A. Nakamura, Nucl. Phys. B584 (2000) 528.

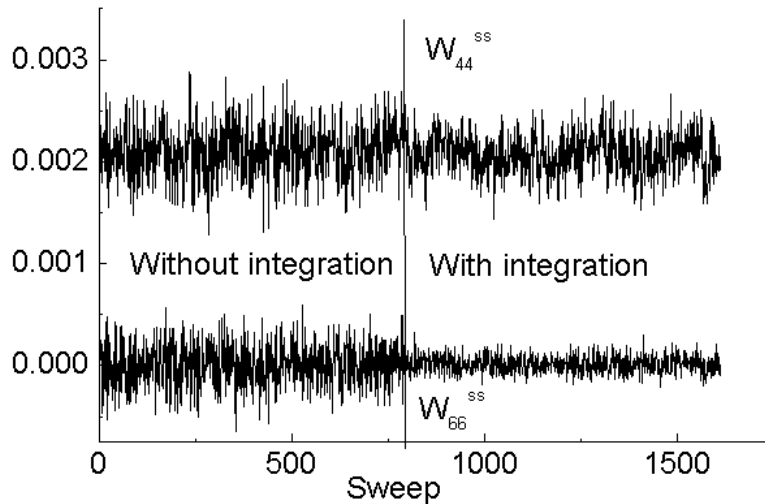


Fig. A.4. An example of the suppression of the fluctuation of Wilson loops for Iwasaki action at  $\beta = 2.5$  and  $\xi_B = 2.0$

- [5] Y. Iwasaki, Nucl. Phys. B258 (1985), 141; Univ. of Tsukuba preprint UTHEP-118 (1983).
- [6] K. Symanzik, Nucl. Phys. B226 (1987) 187  
M. Leuschner and P. Weise, Phys. Lett. B158 (1985) 250.
- [7] QCD-TARO Collaboration Ph. de Forcrand et al., Nucl. Phys. B577 (2000) 263 (hep-lat/9911033).
- [8] G. Parisi, R. Petronzio and F. Rapuano, Phys. Lett. 128B (1983) 418, Nucl. Phys. B205[FS5] (1982) 337.
- [9] R. Brower, P. Rossi and C. I. Tan, Nucl. Phys. B190[FS3] (1981) 699.
- [10] Ph. de Forcrand and C. Roiesnel, Phys. Lett. B31 (1985) 77.
- [11] T. Yoshie, Nucl. Phys. B(Proc Suppl) 63 (1998) 3.
- [12] QCDTARO, private communication.
- [13] G. Cella, G. Curci, A. Vicere and B. Vigna, Phys. Lett. B333 (1994) 457.
- [14] Y. Iwasaki, K. Kanaya, T. Kanenko and T. Yoshie, Nucl. Phys. B(Proc Suppl) 53 (1997) 429.
- [15] A. Nakamura, T. Saito and S. Sakai Nucl. Phys. B(Proc Suppl) 63 (1998) 424.
- [16] Y. Iwasaki and S. Sakai, Nucl. Phys. B248 (1984) 441.
- [17] G. Burgers, F. Karsch, A. Nakamura and I. O. Stamatescu, Nucl. Phys. B304 (1988) 587.

- [18] F. R. Brown and T. J. Woch, Phys. Rev. Letters 58 (1987) 2394.
- [19] M. Creutz, Phys. Rev. D36 (1987) 515. Phys. Rev. Letters 58 (1987) 2394.
- [20] S. Sakai, A. Nakamura and T. Saito, Nucl. Phys. A638 (1998) 535c.
- [21] S. Sakai, A. Nakamura and T. Saito, Nucl. Phys. B(Proc Suppl) 83 (2000) 399.
- [22] G. Martinelli, G. Parisi and R. Petronzio, Phys. Lett. 100B (1981) 435.
- [23] G. P. Lepage and P. B. Mackenzie, Phys. Rev. D48 (1993) 2250.
- [24] T. Scheideler, Dr. thesis, Bielefeld(1997).